

Stationary Fluid Models for the Extra-Planar Gas in Spiral Galaxies

M. Barnabè and L. Ciotti

*Dept. of Astronomy, Bologna University, via Ranzani 1, I-40127
Bologna, Italy*

F. Fraternali

*Theoretical Physics, Oxford University, 1 Keble Road, Oxford OX1
3NP, UK*

R. Sancisi

*INAF-Osservatorio Astronomico di Bologna, via Ranzani 1, I-40127
Bologna, Italy &
Kapteyn Institute, Groningen University, Postbus 800, Groningen,
Netherlands*

Abstract. We show how to construct families of stationary hydrodynamical configurations that reproduce the observed vertical gradient of the rotation velocity of the extra-planar gas in spiral galaxies. We then present a simple model for the lagging halo of the spiral galaxy NGC 891, which is in agreement with the HI observations. Our method is based on the well known properties of baroclinic solutions, and it is an elementary application of a much more general and flexible method.

1. Introduction

Observations at different wavelengths show that spiral galaxies are surrounded by a gaseous halo. This extra-planar gas is multiphase: it is detected in HI (e.g., 452), H α (448), and X-ray observations (454; 450). In particular, high-sensitivity HI observations of edge-on galaxies like NGC 891 (452; 443) and UGC 7321 (446) reveal neutral gas emission up to large distances from the plane and show the presence of a vertical gradient in the gas rotation velocity (see Fig. 1). In addition, the study of face-on galaxies has revealed the presence of vertical motions of neutral gas often associated with holes in the disk HI distribution (447, Boomsma et al., this conference).

Clearly, the two major issues of the origin and of the dynamical state of the extra-planar gas are strictly related. For example, the halo gas could be the result of cosmological accretion (i.e., infall of extragalactic gas; Binney, this conference), or could have been ejected from the plane through a galactic fountain mechanism (451), or it could have had a mixed origin. One might expect different structural and kinematical configurations for these cases. Here we focus on the problem of the dynamical state of the extra-planar gas.

There are two “extreme” kinds of explanations for the extra-planar gas kinematics (low rotation and vertical motions): the ballistic models and the fluid

stationary models. Ballistic models describe the gas as an inhomogeneous collection of clouds in ballistic motion, subjected only to the gravitational potential of the galaxy. A well-known example of ballistic model is the galactic fountain, which describes how ionized gas is ejected from the galactic plane due to stellar winds and supernova explosions and then cools and falls back ballistically onto the disk (439). Ballistic models are effective at explaining vertical motions of the cold (H I) and warm (H α) gas components. However, the observations indicate a considerable morphological and kinematical regularity of the extra-planar gas (see, e.g., the total H I map of NGC 891 in Fraternali et al. 2004 and Fig. 1 here), which may be difficult to understand in the context of purely ballistic models (see also 441).

The observed regularity may be explained more satisfactorily in the context of fluid stationary models. In these models, the gas is taken to be a rotating fluid in stationary equilibrium, without motions along the R and z directions; all the thermodynamical quantities are therefore time-independent, and the galaxy gravitational field is balanced by the pressure gradient and the centrifugal force. Until now, this approach has not been fully explored in all its possibilities, and only a few attempts have been made (e.g., see 436). Here we present a short account of our approach and of its main advantages, while a full discussion will be given in a forthcoming paper (435).

2. Stationary Models: the Standard Approach

The simplest fluid models are constructed by solving the stationary equations of hydrodynamics (written in the standard cylindrical coordinates R , z , and φ), under the assumptions that $v_R = 0$, $v_z = 0$, and $v_\varphi = \Omega R$ (in other words, the system is in a state of *permanent rotation*):

$$\begin{cases} \frac{1}{\rho} \frac{\partial P}{\partial z} = -\frac{\partial \Phi_{\text{tot}}}{\partial z}, \\ \frac{1}{\rho} \frac{\partial P}{\partial R} = -\frac{\partial \Phi_{\text{tot}}}{\partial R} + \Omega^2 R, \end{cases} \quad (1)$$

where ρ , P and Ω are the density, the pressure and the angular velocity of the gas, and Φ_{tot} is the total gravitational potential of the system. Owing to the axial symmetry, all the physical variables are functions of R and z only.

A commonly adopted approach for the solution of Eqs. (1) is that based on the Poincaré-Wavre theorem (445; 453). According to this theorem, the effective gravitational *field* at the r.h.s. of Eqs. (1) can be obtained from an effective *potential* Φ_{eff} if and only if $\Omega = \Omega(R)$. In this case, the gas density, pressure, and temperature are all stratified on Φ_{eff} , the relation between P and ρ is necessarily barotropic [i.e., $P = P(\rho)$], and $v_\varphi = v_\varphi(R)$. The last property, i.e. the so-called “cylindrical rotation”, is in clear disagreement with the observed vertical gradient of the extra-planar gas rotation velocity in spiral galaxies. Thus, in standard applications, one fixes Φ_{tot} and the radial trend of $\Omega(R)$ (thus fixing Φ_{eff}). Then, one solves the equation $\nabla P = -\rho \nabla \Phi_{\text{eff}}$ for the density, with assigned boundary conditions and with specified $P = P(\rho)$; for $\Omega = 0$ one recovers the standard (barotropic) hydrostatic equilibrium solutions.

Clearly, rotational velocities changing with z are excluded here, and this would seem to argue against the fluid stationary approach.

However, in the next Section we will show that it is possible to construct *baroclinic* equilibrium solutions with a negative velocity gradient along z : this approach is a simple application of a more general technique that will be presented by Barnabè et al. (435). Note that baroclinic solutions have been studied before for problems ranging from geophysics to the theory of sun spots to galactic dynamics (e.g., see 449; 453; 455, and references therein). In particular, isotropic, self-gravitating axisymmetric galaxy models can be interpreted as baroclinic fluid configurations, showing streaming velocities often decreasing with z (e.g., see 444).

3. Stationary Models: Baroclinic Solutions

At variance with the standard approach, here we start by assuming a gas density distribution $\rho(R, z)$ (vanishing at infinity). Thus, for a given $\Phi_{\text{tot}}(R, z)$, the first of Eqs. (1) can be integrated to obtain the gas pressure

$$P(R, z) = \int_z^\infty \rho \frac{\partial \Phi_{\text{tot}}}{\partial z'} dz'. \quad (2)$$

In general, P can not be expressed as a function of ρ only, and so our system is barocline. Its temperature distribution is obtained from the perfect gas equation of state,

$$T = \frac{\mu m_H P}{k \rho}. \quad (3)$$

Inserting Eq. (2) in the second of Eqs. (1) and integrating by parts one obtains a remarkable “commutator-like” expression for the rotational velocity

$$\frac{\rho v_\varphi^2}{R} = \int_z^\infty \left(\frac{\partial \rho}{\partial R} \frac{\partial \Phi_{\text{tot}}}{\partial z'} - \frac{\partial \rho}{\partial z'} \frac{\partial \Phi_{\text{tot}}}{\partial R} \right) dz'. \quad (4)$$

Clearly, due to the baroclinic nature of the solution, the quantity v_φ will depend on z . Unfortunately, the construction of barocline solutions is not as easy as it appears: in fact, not all the density distributions produce *physically acceptable* solutions, that is solutions for which $v_\varphi^2 \geq 0$ everywhere. However, using Eq. (4) we can state a few sufficient conditions that can be used as *guidelines* to choose the density distribution ρ and to obtain physically acceptable solutions. From now on, for simplicity we assume that the gas is not self-gravitating. Two sufficient conditions are the following:

- (i) when the total potential is homeoidally stratified with axial ratio q_Φ , i.e.

$$\Phi_{\text{tot}} = \Phi_{\text{tot}}(\ell), \quad \ell^2 \propto R^2 + \frac{z^2}{q_\Phi^2}, \quad 0 < q_\Phi \leq 1, \quad (5)$$

(as in Binney’s [1991] logarithmic potential and Evans’ [1994] spheroidal potentials), if one assume a gas density distribution of the form

$$\rho(R, z) = \rho_1(R)\rho_2(m), \quad m^2 \propto R^2 + \frac{z^2}{q_g^2}, \quad 0 < q_g \leq 1, \quad (6)$$

a sufficient condition to have $v_\varphi^2 \geq 0$ everywhere is

$$\frac{d\rho_1(R)}{dR} \geq 0, \quad \frac{d\rho_2(m)}{dm} \leq 0, \quad \text{and} \quad q_g \leq q_\Phi. \quad (7)$$

In particular, the third condition requires the gas density distribution to be stratified on *flatter* homeoids than the equipotentials.

- (ii) When the total potential is generated by a razor thin uniform disk, (i.e. $\Phi_{\text{tot}} = 2\pi G\Sigma_0 z$), a necessary and sufficient condition to obtain $v_\varphi^2 \geq 0$ everywhere is $\partial\rho(R, z)/\partial R \geq 0$.

In particular, point (ii) suggests that if the stellar disk contribution to the total potential is dominant in the central regions, a “sufficient condition” to have physically acceptable solutions is to take a centrally depressed gas distribution. The physical reason for this condition is very simple. In fact, imagine a generic $\rho(R, z)$ distribution in a uniform (vertical) gravitational field. The gas distribution is not stratified on Φ_{tot} and so must be rotating. According to the second of Eq. (1) this means that, at any fixed z , the gas pressure must increase with R . This requirement can be stated in terms of the gas column density $\int_z^\infty \rho dz'$. In fact from Eq. (4) it follows that in a vertical gravitational field the square of the gas rotational velocity is just proportional to the radial gradient of the column density, which must be positive. It is worth mentioning that this trend is consistent with the observed HI surface density distribution for several spiral galaxies (see 440).

4. A Simple Model for the NGC 891 Lagging Halo

As a simple application of baroclinic solutions we have attempted to reproduce the observed negative gradient of the rotational velocity of the extra-planar gas in NGC 891. The model here should be considered exploratory, in the sense that we are not interested at reproducing the kinematical data in detail, but only to provide a reasonable, physically acceptable model for the extra-planar gas, and to show that baroclinic solutions deserve deeper investigations in the context of the extra-planar gas kinematics.

We consider a very simple galaxy model that consists of two components, namely a razor-thin exponential stellar disk

$$\Phi_{\text{disk}}(R, z) = -\frac{GM_d}{R_d} \int_0^\infty \frac{J_0(k\tilde{R})e^{-k|\tilde{z}|}}{(1+k^2)^{3/2}} dk, \quad \tilde{R} \equiv \frac{R}{R_d}, \quad \tilde{z} \equiv \frac{z}{R_d}, \quad (8)$$

and a logarithmic dark matter halo (437) with constant asymptotic velocity v_0

$$\Phi_{\text{halo}}(R, z) = \frac{v_0^2}{2} \ln \left(\tilde{R}_h^2 + \tilde{R}^2 + \frac{\tilde{z}^2}{q_h^2} \right), \quad \tilde{R}_h \equiv \frac{R_h}{R_d}. \quad (9)$$

The galaxy bulge is not considered here. In Eqs. (8)-(9) M_d and R_d are the disk mass and scale radius, R_h and q_h are the halo potential scale radius and

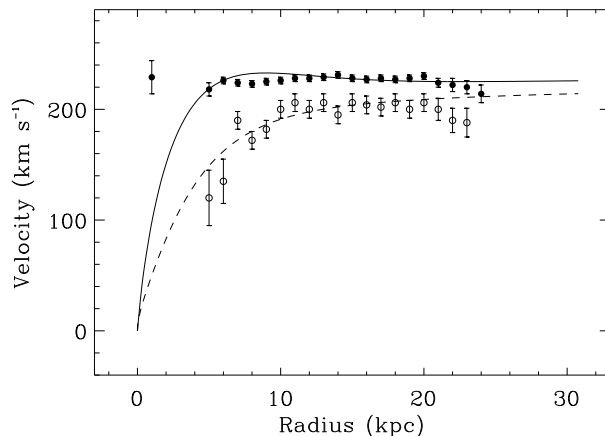


Figure 1. Rotation curve of NGC 891 for the gas in the plane of galaxy (*filled circles*) and for a strip from 30'' to 60'', corresponding to about 2.25 kpc, above and below the plane (*open circles*). The solid curve represents the circular velocity in the equatorial plane of the model galaxy, while the dashed curve is the rotational velocity of the baroclinic solution 2.25 kpc above the galactic plane.

flattening parameter, and J_n is the n -th order Bessel function of the first kind (e.g., 438).

Following the simple criteria illustrated in points (i) and (ii), we adopted the trial function

$$\rho(R, z) = \frac{\rho_0}{R_0^\alpha} \frac{(R_0 + R)^\alpha}{(1 + m^2)^{\beta/2}} e^{-(\tilde{z}/h_g)^\gamma}, \quad m^2 \equiv \tilde{R}^2 + \frac{\tilde{z}^2}{q_g^2}, \quad (10)$$

where ρ_0 , R_0 and h_g are the central density, the radial and vertical scales of the gas distribution, and α , β and γ are dimensionless constants. For $\alpha > 0$, Eq. (10) describes a centrally depressed (i.e. toroidal) gas density distribution, and the exponential is a scale-height modulating function. Note that the equations for this model must be solved numerically, and the description of the code will be given in Barnabè et al. (435). After a few attempts we fixed $R_d = 3$ kpc, $M_d = 8 \times 10^{10} M_\odot$, $v_0 = 220$ km s $^{-1}$, $\tilde{R}_h = 5$, $q_h = 0.71$, $R_0 = 2$ kpc, $h_g = 3/2$, $\alpha = 1$, $\beta = 4$, $\gamma = 1/2$ and $q_g = 1/4$. For this choice the model circular velocity reproduces the observed rotation curve of NGC 891 (see Fig. 1, solid line), and $v_\phi^2 \geq 0$ everywhere. According to Eqs. (3)-(4), the quantities v_ϕ and T do not depend on the value of ρ_0 .

The meridional section of the iso-rotation surfaces are shown in Fig. 2 as solid lines: v_ϕ decreases with z over the main body of the distribution, with the exception of the region $R \lesssim 2R_d$ and $z \sim 0$, where v_ϕ varies in a non-monotonic way with z .

The dashed curve in Fig. 1 corresponds to a horizontal cut of Fig. 2, at $z \simeq 2.25$ kpc, superimposed to the observed values of the HI rotation velocity at the same z . The match between the observed points and the model curve is surprisingly good, in particular when considering the exploratory nature of the presented model.

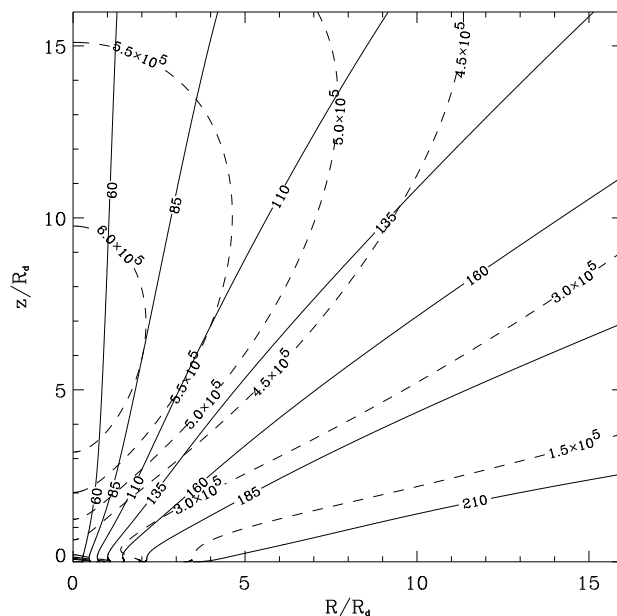


Figure 2. Meridional section of iso-rotation (*solid*, in km s^{-1}) and isothermal (*dashed*, in Kelvins) surfaces for the model in Eqs. (8)-(10).

The model isothermal surfaces are also shown in Fig. 2 as dashed lines. As expected, the gas distribution is quite hot, with temperatures in the range $10^5 \lesssim T \lesssim 10^6$ K. The hotter region is a “bubble” near the symmetry axis above (and below) the equatorial plane, while the gas temperature decreases steadily approaching the galactic disk. In Barnabè et al. (435) we present and discuss the (soft) X-ray total luminosity and surface brightness maps of our models. In order to compare the model with the observations the value for the central gas density, ρ_0 , must be known. In fact, one could proceed as follows: while the dimensionless part of Eq. (10) can be fixed to reproduce the rotational and temperature fields, the observed total X-ray luminosity could be used to determine ρ_0 . With this parameter fixed, one can then discuss other, astrophysically relevant model properties (see next Section).

5. Discussion and Conclusions

We have presented fluid models for the extra-planar gas in spiral galaxies. The approach is based on the class of hydrodynamical equilibria known as baroclinic solutions. In particular, we have shown how very simple baroclinic configurations can be characterized by a decrease of rotational velocity with increasing z similar to that observed in the extra-planar gas of spiral galaxies. We remark that baroclinic solutions are very flexible: for instance, if we require v_φ to reach the systemic velocity for large $|z|$ (i.e., the halo becomes hydrostatic), one could repeat the previous analysis with a factorized gas density distribution as $\rho(R, z) = f(R, z)\rho_e(\Phi_{\text{tot}})$, where $f \sim 1$ at large $|z|$ and ρ_e is an hydrostatic equilibrium solution in the galactic potential. Even more general cases can

be obtained by “perturbing” a cylindrical rotation solution, i.e., by assuming $\rho_e = \rho_e(\Phi_{\text{eff}})$. For such distributions several interesting results similar to those reported in points (i) and (ii) can be easily derived (435).

We conclude by discussing the major limitations and open problems related to the use of a fluid approach:

1) Homogeneity. Observationally the gas is multiphase: what is the relationship between the (hot) single-phase gas described by fluid models and the H I and H α components of extra-planar gas?

2) Absence of vertical motions. Observations show vertical motions of the order of 50 – 100 km/s, while in the approach described in Sect. 3 such motions are excluded: is this enough reason to abandon stationary fluid solutions?

About point 1), a first important insight will be given by the calculation, for a chosen baroclinic distribution, of the *local* and *global* cooling times. In fact, while the global cooling time sets the rate at which heat must be furnished to the distribution in order to assure stationarity, the local cooling time indicates where clouds will condense out of the smooth density distribution. It would be interesting to follow the trajectories of such falling clouds under the drag force of the gas and with initial conditions given by the baroclinic solution. Thermal conduction could be another important ingredient in the evolution of the clouds. Of similar interest would be the study of the interaction of cosmologically accreted cold gas with a hot rotating halo. In particular, it would be interesting to measure evaporation times and to find out whether and on what time-scales the kinematic regularity of the fluid solution is transferred to the infalling cloud population.

As to point 2), in addition to the comments above, we also note that baroclinic solutions can be generalized to include meridional motions. This generalization is not trivial but can be obtained, at least in the geostrophic limit (i.e., for small Rossby numbers), by standard expansion techniques (e.g., 455; 453). Numerical methods are required to investigate existence and properties of solutions with faster meridional motions. In any case, it cannot be excluded that meridional motions may also play a role in the kinematics of the hot gas.

Thus, it is clear that the ballistic and fluid approaches both give important (but restricted) information about the state of the extra-planar gas. A better understanding of the problem will be obtained by the investigation of the interaction of clouds with baroclinic fluid configurations using time-dependent numerical hydrodynamical simulations. Numerical simulations will also clarify the fate of the “torus-like” structure common in baroclinic distributions.

References

- Barnabè, M., Ciotti, L., Fraternali, F., & Sancisi, R. 2004, in preparation
 Benjamin, R. A. 2002, in ASP Conf. Ser. Vol. 276, Seeing Through the Dust: the Detection of H I and the Exploration of the ISM in Galaxies, ed. A. R. Taylor, T. L. Landecker & A. G. Willis (San Francisco: ASP), 201
 Binney, J. 1981, MNRAS, 196, 455
 Binney, J. & Tremaine, S. 1987, Galactic Dynamics (Princeton: Princeton University Press)
 Bregman, J. N. 1980, ApJ, 236, 577
 Cayatte, V., Kotanyi, C., Balkowski, C., & van Gorkom, J. H. 1994, AJ, 107, 1003
 Collins, J. A., Benjamin, R. A., & Rand, R. J. 2002, ApJ, 578, 98

- Evans, N. W. 1994, *MNRAS*, 267, 333
- Fraternali, F., Oosterloo, T., Boomsma, R., Swaters, R., & Sancisi, R. 2004, in *IAU Symp. 217, Recycling Intergalactic and Interstellar Matter*, eds. P.-A. Duc, J. Braine & E. Brinks (Sidney: IAU), 136
- Lanzoni, B. & Ciotti, L. 2003, *A&A*, 404, 819
- Lebovitz, N. R. 1967, *ARA&A*, 5, 465
- Matthews, L. D. & Wood, K. 2003, *AJ*, 593, 721
- Puche, D., Westpfahl, D., Brinks, E., & Roy, J.-R. 1992, *AJ*, 103, 1841
- Rand, R. J. 2000, *ApJ*, 537, L13
- Rosseland, S. 1926, *ApJ*, 63, 342
- Strickland, D. K., Heckman, T. M., Colbert, E. J. M., Hoopes, C. G., & Weaver, K. A. 2004, *ApJS*, 151, 193
- Shapiro, P. R. & Field, G. B. 1976, *ApJ*, 205, 762
- Swaters, R. A., Sancisi, R., & van der Hulst, J. M. 1997, *ApJ*, 491, 140
- Tassoul, J.-L. 1980, *Theory of Rotating Stars* (Princeton: Princeton University Press)
- Wang, Q. D., Immler, S., Walterbos, R., Lauroesch, J. T., & Breitschwerdt, D. 2001, *ApJ*, 555, L99
- Waxman, A. M. 1978, *ApJ*, 222, 61